

# MHD Equilibrium Analysis with Anisotropic Pressure in LHD<sup>\*</sup>)

Yoshimitsu ASAHI<sup>1)</sup>, Yasuhiro SUZUKI<sup>1,2)</sup>, Kiyomasa WATANABE<sup>1,2)</sup> and Wilfred A. COOPER<sup>3)</sup>

<sup>1)</sup>The Graduate University for Advanced Studies, 322-6 Oroshi-cho, Toki 509-5292, Japan

<sup>2)</sup>National Institute for Fusion Science, 322-6 Oroshi-cho, Toki 509-5292, Japan

<sup>3)</sup>Ecole Polytechnique Fédérale de Lausanne, Centre de Recherches en Physique des Plasmas, Association Euratom-Suisse, CH1015 Lausanne, Switzerland

(Received 23 December 2010 / Accepted 9 May 2011)

The effects of anisotropic pressure on MHD equilibrium are investigated, particularly focused on the position of the magnetic axis. MHD equilibria are numerically calculated under anisotropic pressure conditions using an extension of the VMEC code which is widely applied to obtain three dimensional MHD equilibria. This code is called ANIMEC. A bi-Maxwellian model was invoked in this code in order to treat anisotropic pressure driven by energetic particles without any inconsistency. To investigate the properties of the plasma with  $p_{\parallel} > p_{\perp}$ , numerical computations under various conditions are performed with a LHD magnetic configuration using the ANIMEC code. Comparisons of the plasma behavior between an analytical model that considers  $p_{\parallel}$  and  $p_{\perp}$  to be constant on each flux surface and ANIMEC numerical results will be discussed.

© 2011 The Japan Society of Plasma Science and Nuclear Fusion Research

Keywords: MHD equilibrium, anisotropic pressure, high-beta plasma, LHD

DOI: 10.1585/pfr.6.2403123

## 1. Introduction

In LHD experiments, high beta plasmas with more than 5% volume averaged beta are obtained without any disruptive phenomena. This beta value is relevant and requisite as a design criterion for fusion reactor systems.

High  $\beta$  plasmas in LHD experiments are generated and maintained only by tangentially injected neutral beams (NB) with low density and low magnetic field. The high energy ions from the tangential NB are well confined even when the magnetic field is low. Because of the long slowing down time of high energy particles in low density regimes and the low thermal pressure due to the low magnetic field, the beam pressure cannot be ignored compared with the thermal pressure. As a result, it is expected to cause an anisotropy in the pressure with parallel component along the equilibrium magnetic field lines  $p_{\parallel}$  greater than  $p_{\perp}$ , its perpendicular counterpart. Figure 1 shows the time evolution of the beta value in a typical LHD high  $\beta$  discharge with the assumption that the pressure is isotropic. According to the evaluation of the beam pressure, which is based on a Monte-Carlo analysis, 30% of the total plasma pressure corresponds to the contribution from the fast beam pressure ions [1].

Until now, simulations of MHD equilibria with the anisotropic pressure conditions achieved in LHD experiments have not been undertaken. The final goal is to establish an identification method of the MHD equilibria achieved in LHD experiments. In this paper, we concentrate our investigations on effects of anisotropic pres-

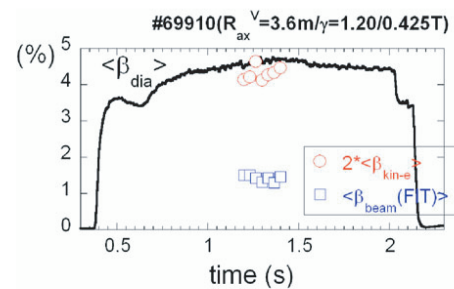


Fig. 1 Time evolution of beta values in a typical LHD high beta discharge. The beta value estimated from diamagnetic flux measurements is shown with the solid line and from  $n_e$  and  $T_e$  profile measurements with red circles, with the assumption that the pressure is isotropic. The blue square points indicate the estimated beam beta value obtained by Monte-Carlo calculations.

sure in MHD equilibrium computations. Recently, a three-dimensional MHD equilibrium analysis code was developed [2], in which a bi-Maxwellian model was implemented in the VMEC code to enable anisotropic pressure treatments. Using this code, the impact of the magnetic axis position dependence on anisotropic pressure has been investigated in the LHD configuration with  $p_{\parallel} > p_{\perp}$  plasmas.

## 2. Previous Analytic Model

An analytical expression of the magnetic axis shift with anisotropic pressure is presented here. Stellarator plasma equilibria with anisotropic pressure were studied

author's e-mail: asahi.yoshimitsu@nifs.ac.jp

<sup>\*</sup>) This article is based on the presentation at the 20th International Toki Conference (ITC20).

by Hitchon *et al.* [3, 4] which is based on a low-beta ordering [5];  $\beta \sim O(\epsilon^2)$  and the CGL formula [6];  $p = p_{\perp} I + (p_{\parallel} - p_{\perp}) \mathbf{nn}$ . Here,  $\epsilon$  is the inverse aspect ratio,  $p_{\parallel}$  and  $p_{\perp}$  are pressure components parallel and perpendicular to magnetic field,  $I$  is the unit tensor and  $\mathbf{n}$  is the unit vector along the magnetic field. In this framework, the leading terms of  $p_{\parallel}$  and  $p_{\perp}$  are functions of only the magnetic flux surface, and these are defined as  $P_{\parallel}$  and  $P_{\perp}$ , respectively. In this case, the Pfirsch-Schlüter current can be expressed as [3, 7]

$$j_{PS} = \frac{\rho}{b^*} (P'_{\parallel} + P'_{\perp}) \cos \theta, \quad (1)$$

and in the case isotropic pressure,

$$j_{PS} = \frac{\rho}{b^*} p' \cos \theta, \quad (2)$$

where  $\rho = r/a$ ,  $' = \partial/\partial\rho$  and  $\theta$  is the poloidal angle. The variables used in the above equations are defined in Ref. [3, 8].

### 3. Calculation Model

The MHD equilibrium study in LHD has been done mainly with the VMEC code, which assumes that plasmas have isotropic pressure. Recently, the VMEC code was extended by Cooper *et al.* to be able to treat anisotropic pressure, and this version of VMEC is referred to as the ANIMEC code [2].

By introducing a bi-Maxwellian model [9], the ANIMEC code is capable of identifying anisotropic pressure MHD equilibria without inconsistency. The velocity distribution function of energetic particles is expressed as follows,

$$F_h(s, \epsilon, \mu) = N(s) \left( \frac{m_h}{2\pi T_{\perp}(s)} \right)^{\frac{3}{2}} \times \exp \left[ -m_h \left( \frac{\mu B_C}{T_{\perp}(s)} + \frac{|\epsilon - \mu B_C|}{T_{\parallel}(s)} \right) \right], \quad (3)$$

where  $s$  is the radial index,  $N(s)$  is the label of the density-like amplitude factor,  $\epsilon$  is the kinetic energy,  $m_h$  is the mass of the high-energy particles, and  $T_{\parallel}$  and  $T_{\perp}$  are the temperatures of high energy particles in the direction parallel and perpendicular to magnetic field. Then the total parallel pressure is expressed as

$$p_{\parallel}(s, B) = M(s) (1 + p_h(s) H(s, B)). \quad (4)$$

Here, the  $H(s, B)$  factor describes the variation of the pressure distribution around the flux surfaces caused by the energetic trapped particles. The plasma region where  $B > B_C$

$$H(s, B) = \frac{B/B_C}{1 - \frac{T_{\perp}}{T_{\parallel}} \left( 1 - \frac{B}{B_C} \right)}, \quad (5)$$

and where  $B < B_C$ ,

$$H(s, B) = \frac{B}{B_C} \frac{1 + \frac{T_{\perp}}{T_{\parallel}} \left( 1 - \frac{B}{B_C} \right) - 2 \left( \frac{T_{\perp}}{T_{\parallel}} \right)^{\frac{5}{2}} \left( 1 - \frac{B}{B_C} \right)^{\frac{5}{2}}}{\left[ 1 - \frac{T_{\perp}}{T_{\parallel}} \left( 1 - \frac{B}{B_C} \right) \right] \left[ 1 + \frac{T_{\perp}}{T_{\parallel}} \left( 1 - \frac{B}{B_C} \right) \right]}. \quad (6)$$

By choosing the value  $B_C$  to be smaller than the minimum magnetic field strength in the plasma confinement region, calculations which exclude the effect of energetic trapped particles can be performed.

The MHD equilibrium analysis code VMEC and its ANIMEC extension identifies the shape of the flux surfaces using a variational plasma energy  $W$  minimizing principle. In the case that pressure is isotropic, the plasma energy functional is written as

$$W = \int dV \left( \frac{B^2}{2\mu_0} + \frac{p}{\Gamma - 1} \right). \quad (7)$$

However, in the case of anisotropic,  $W$  is written as follows,

$$W = \int dV \left( \frac{B^2}{2\mu_0} + \frac{p_{\parallel}(s, B)}{\Gamma - 1} \right). \quad (8)$$

The pressure perpendicular to field  $p_{\perp}$  is estimated from parallel force balance relation [10], hence

$$p_{\perp}(s, B) = p_{\parallel}(s, B) - B \frac{\partial p_{\parallel}}{\partial B} \Big|_s. \quad (9)$$

Equations (8) and (9) are used in the ANIMEC code.

Pressure components  $p_{\parallel}$  and  $p_{\perp}$  from the bi-Maxwellian velocity distribution function model invoked are not constant in each flux surface. Typical profiles of  $p_{\parallel}$  and  $p_{\perp}$  corresponding to the LHD vertically elongated cross-section are shown in Fig. 2 in the situation that the parallel component is larger than the perpendicular one. Figures 2(a) and (b) is an example of the result without trapped particles. In this calculation,  $B_C$  is set to 0.24 [T], which is lower than the minimum magnetic field. In fact, the minimum field strength is 0.30 [T] in the plasma region. An example in which trapped particles effects are taken into account is modeled in Figs. 2(c) and (d). Here we chose,  $B_C = 0.60$  [T]. These are obtained by setting  $T_{\perp}/T_{\parallel} = 0.1$ ,  $p_h = 3$ ,  $\Gamma = 0$ ,  $M(s) = m_0(1 - s)$  in regard to the equations (4), (5) and (6). Each pressure value  $p_{\parallel}$  and  $p_{\perp}$  is normalized to its respective maximum value  $p_{\parallel}^{\text{Max}}$  and  $p_{\perp}^{\text{Max}}$ . In Figs. 2(b) and (d), there is no symbol in the vicinity of  $\rho_{\text{Equatorial}} = 0$  because the ANIMEC code uses half-integer radial mesh discretization and there is consequently no data at the magnetic axis.

### 4. Numerical Results from the Bi-Maxwellian Model

To investigate effects of anisotropic pressure with respect to the magnetic axis shift, a large number of numerical calculations are performed under various conditions using the ANIMEC code. In these simulations, the pressure profile  $M(s)$  is given as  $M(s) = m_0(1 - s)$  where  $s = \rho^2$ . The maximum pressure (at the magnetic axis) corresponds to  $m_0$ . The values of  $m_0$  chosen are 0.5, 1.0, 1.5,  $\dots \times 10^3$  [Pa] and  $T_{\perp}/T_{\parallel}$  is given the [0, 1] range. The ratio of specific heats  $\Gamma$  in Eq. (8) and (7) is set to zero for simplicity, which corresponds to the limit of incompressibility.

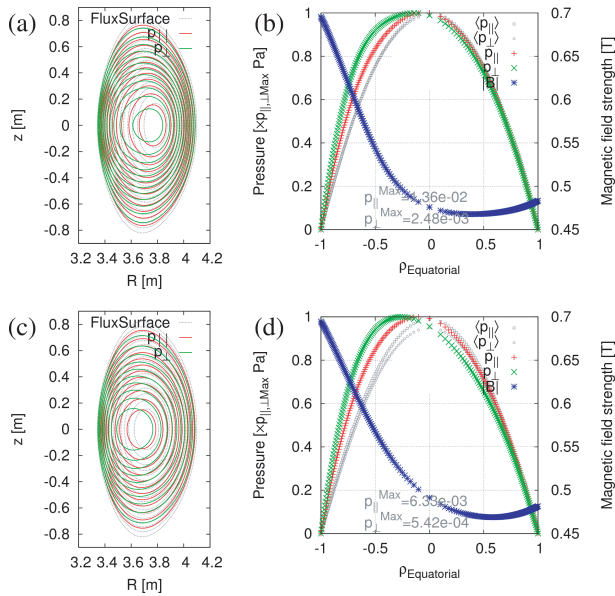


Fig. 2 Pressure contours of  $p_{\parallel}$  and  $p_{\perp}$  components without trapped particles (top row) and with trapped particles (bottom row) in the LHD vertically elongated cross-section (a, c) and its profile along the  $z = 0$  line (b, d) obtained with the bi-Maxwellian model. In figures (a) and (c), the red and the green curves denote  $p_{\parallel}$  and  $p_{\perp}$  contours and the shape of the flux surfaces are shown with gray dotted lines. In figures (b) and (d), the red and the green symbols denote  $p_{\parallel}$  and  $p_{\perp}$  profiles and the gray symbols denote the flux surface averaged value.

First of all, we define two  $\beta$  values under anisotropic pressure. One is the total beta value which is estimated from the plasma energy and the principle of equipartition of energy.

$$\beta_{\text{tot}} = \frac{\frac{1}{3} \int dV (p_{\parallel} + 2p_{\perp})}{\int dV \left( \frac{B^2}{2\mu_0} \right)}. \quad (10)$$

The other is the value expected to yield the equivalent magnitude of axis shift compared with isotropic pressure equilibria. Focusing on the dependence of the Pfirsch-Schlüter current on the pressure components in Eq. (1), which is the result of the earlier analytic model [3, 4], we define the equivalent beta value as

$$\beta_{\text{eq}} = \frac{\frac{1}{2} \int dV (p_{\parallel} + p_{\perp})}{\int dV \left( \frac{B^2}{2\mu_0} \right)}. \quad (11)$$

Note that these two  $\beta$  values defined above are identical when a plasma has isotropic pressure  $p_{\perp} = p_{\parallel}$ .

The relation between the beta values and the magnetic axis position is shown in Figs. 3-5. The points with green, blue, pink, light blue colored correspond to the different value  $m_0 = 0.5, 1.0, 1.5, 2.0$  [ $\times 10^3$  Pa] with  $T_{\perp}/T_{\parallel} = [0, 1]$  of Eqs. (4)-(6) in the computations.

As shown in Figs. 3-5, the magnetic axis shift is proportional to  $\beta_{\text{eq}}$  rather than  $\beta_{\text{tot}}$ . The amount of magnetic

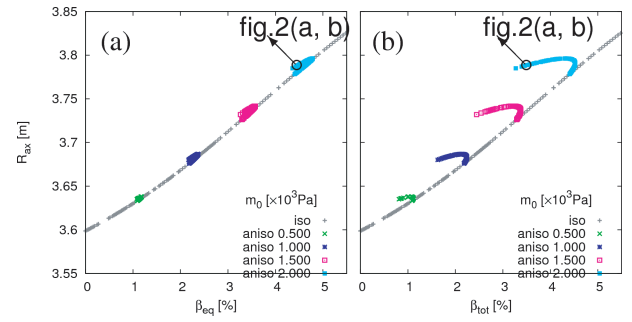


Fig. 3 The dependence of the magnetic axis position on the beta value obtained from calculations with trapped particle effects neglected. The horizontal axes in each figure are denoted by  $\beta_{\text{tot}}$  or  $\beta_{\text{eq}}$ . The gray points correspond to the isotropic pressure plasma axis positions which  $T_{\perp}/T_{\parallel} = 1$ .

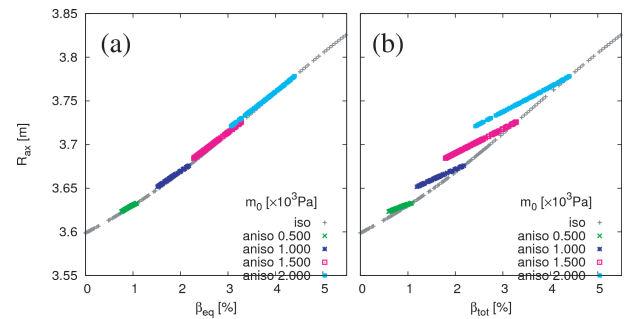


Fig. 4 The dependence of the magnetic axis position on the beta value obtained from calculations with a small fraction of trapped particles.

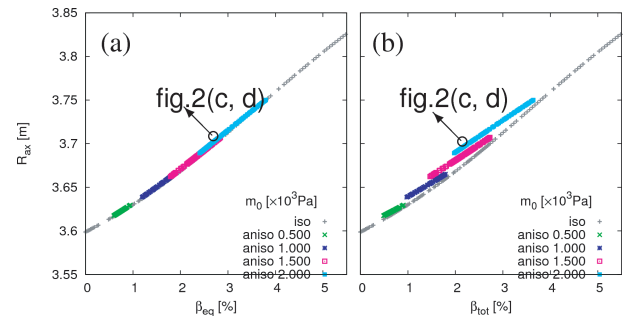


Fig. 5 The dependence of the magnetic axis position on the beta value obtained from calculations with a large fraction of trapped particles.

axis shift depends on the Pfirsch-Schlüter current. Because  $\beta_{\text{tot}}$  and  $\beta_{\text{eq}}$  are the indices of the internal energy of the plasma and the Pfirsch-Schlüter current, respectively, the amount of axis shift is proportional to  $\beta_{\text{eq}}$ . On the contrary for the case that plasma pressure is isotropic, the two indices are identical;  $\beta_{\text{tot}} = \beta_{\text{eq}}$ . Thus, the axis shifts of the anisotropic pressure and the isotropic pressure equilibria have the same dependence on  $\beta_{\text{eq}}$ .

As seen from Fig. 3 (b), magnetic axis appears to be a multi function of  $\beta_{\text{tot}}$ . In this calculation,  $T_{\perp}/T_{\parallel}$  varies

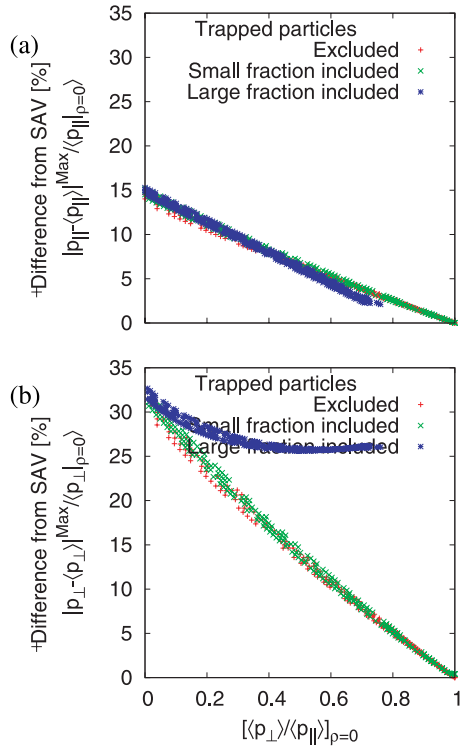


Fig. 6 The maximum absolute value of the difference between the parallel pressure and its flux surface average normalized to its average value on axis (a) and the corresponding maximum absolute value for the perpendicular pressure (b) as a function of the ratio of  $\langle p_{\perp} \rangle$  to  $\langle p_{\parallel} \rangle$  corresponding to the strength of the anisotropy at the magnetic axis. Here,  $\langle A \rangle$  means the surface averaged of the quantity  $A$ . The three different kind of points plotted highlight the impact of the energetic trapped particle fraction. The red '+' points correspond to simulations in which trapped particle effects are excluded. The green 'x' points and the blue '\*' points correspond to conditions of small and large trapped particle fractions included, respectively, in the low magnetic field region of the plasma.

from zero to unity for each  $m_0$  value as shown before, without holding either  $\beta_{\text{tot}}$  or  $\beta_{\text{eq}}$  fixed. The form

$$\beta_{\text{eq}} = \frac{3}{2}\beta_{\text{tot}} - \frac{1}{2}\beta_{\perp} = \frac{3}{2}\beta_{\text{tot}}\beta_{\parallel} \left( \frac{1 + \beta_{\perp}/\beta_{\parallel}}{1 + 2\beta_{\perp}/\beta_{\parallel}} \right) \quad (12)$$

with

$$\beta_{\parallel} = \frac{\int dV p_{\parallel}}{\int dV \left( \frac{B^2}{2\mu_0} \right)}, \quad \beta_{\perp} = \frac{\int dV p_{\perp}}{\int dV \left( \frac{B^2}{2\mu_0} \right)}, \quad (13)$$

means that  $\beta_{\text{eq}}$  can vary with different ratios of  $\beta_{\perp}/\beta_{\parallel}$  even for  $\beta_{\text{tot}}$  constant. Modifications of the  $T_{\perp}/T_{\parallel}$  ratio induce changes in  $\beta_{\parallel}$  and  $\beta_{\perp}$ . Thus the magnetic axis can have multiple values in terms of  $\beta_{\text{tot}}$  because the position of the magnetic axis is uniquely identified by  $\beta_{\text{eq}}$ .

Figure 6 illustrates the maximum absolute difference

between the surface averaged pressure value and its normal value as a function of the anisotropy. The maximum of this difference is estimated in the vertically elongated cross-section. Figures 6 (a) and (b) show the variations of  $p_{\parallel}$  and  $p_{\perp}$ , respectively. As the results include different values of  $m_0$  like 0.5, 0.1, 1.5, 2.0 [ $\times 10^3$  Pa] plotted simultaneously, there is the appearance of a multi-valued dependence  $[\langle p_{\perp} \rangle / \langle p_{\parallel} \rangle]_{\rho=0}$ . For the case of a large trapped particle fraction, the abscissa value  $[\langle p_{\perp} \rangle / \langle p_{\parallel} \rangle]_{\rho=0}$  is smaller than unity even when  $T_{\perp}/T_{\parallel} = 1$ . This is caused by the anisotropy of the velocity distribution function because the value  $B_c/B$  can become larger than unity. Here, ' $\langle \rangle$ ' means the averaged value on a flux surface. Figure 6 implies that the difference in the variation of the pressures around the flux surfaces needs to grow as the anisotropy  $[\langle p_{\perp} \rangle / \langle p_{\parallel} \rangle]_{\rho=0}$  factor decrease in order to satisfy equilibrium force balance. Particularly for  $p_{\perp}$  component, in the case that the trapped particle fraction exists in a large domain of the low magnetic field region, this difference needs to remain large even when  $[\langle p_{\perp} \rangle / \langle p_{\parallel} \rangle]_{\rho=0}$  is nearly equal to unity.

## 5. Summary

MHD equilibria with anisotropic pressure plasma are analyzed in a LHD magnetic configuration. Here, we assume the pressure is based on a bi-Maxwellian distribution function model whose moments are nonconstant on each flux surface. We have focused on the magnetic axis shift due to the anisotropic pressure with a large parallel component that would be consistent with the fast ions from tangential neutral beam injection. As the result, the change of the axis position depends on the pressure anisotropy, but does not depend on the difference of the pressure from its averaged value on each flux surface. The results from an analytic model which assumes constant pressure on each flux surface coincide with those from our numerical analysis based on a bi-Maxwellian model. A study of the reason why the two models have comparable magnetic axis shifts constitutes a subject for future research.

- [1] K.Y. Watanabe *et al.*, Fusion Science and Technology **58**, 160 (2010).
- [2] W.A. Cooper *et al.*, Comp. Phys. Comm. **180**, 1524 (2009).
- [3] W.N.G. Hitchon *et al.*, Nucl. Fusion **23**, 383 (1983).
- [4] W.N.G. Hitchon *et al.*, Nucl. Fusion **21**, 775 (1981).
- [5] J.M. Greene and J.L. Johnson, Phys. Fluids **4**, 875 (1961).
- [6] G.F. Chew *et al.*, Proceedings of the Royal Society of London Series A (Mathematical and Physical Sciences) **236**, 112 (1956).
- [7] V.D. Pustovitov, Plasma Phys. Control. Fusion **52**, 1 (2010).
- [8] P.J. Fielding and W.N.G. Hitchon, Plasma Phys. **24**, 453 (1980).
- [9] K.G. McClements *et al.*, Phys. Plasmas **3**, 2994 (1996).
- [10] W.A. Cooper *et al.*, Comp. Phys. Comm. **72**, 1 (1992).